ACS OMEGA

http://pubs.acs.org/journal/acsodf

Article

Facile Chemical Synthesis of Co−Ru-Based Heterometallic Supramolecular Polymer for Electrochemical Oxidation of Bisphenol A: Kinetics Study at the Electrode/Electrolyte Interface

Abdul Awal,[§] Santa Islam,[§] Tamanna Islam, Md. Mahedi Hasan, S. M. Abu Nayem, Md. Mahmudul Haque James, Md. Delwar Hossain,* and A. J. Saleh Ahammad*

Cite This: *ACS Omega* 2023, 8, 28355−28366

Read Online

ACCESS | Metrics & More | Article Recommendations | Supporting Information

ABSTRACT: Regardless of the adverse effects of Bisphenol A (BPA), its use in industry and in day-to-day life is increasing at a higher rate every year. In the present study, a simple and reliable chemical approach was used to develop an efficient BPA sensor based on a Co−Ru-based heterometallic supramolecular polymer (polyCoRu). Surface morphology and elemental analysis were examined using scanning electron microscopy (SEM) and energy-dispersive X-ray spectroscopy (EDX). Furthermore, functional group analysis was accomplished by Fourier transform infrared spectroscopy (FT-IR). UV−vis spectroscopy was used to confirm the complexation in the ratio of 0.5:0.5:1 (metal 1/metal 2/ligand). Electrochemical characterization of the synthesized polyCoRu was conducted using cyclic voltammetry (CV) and electrochemical impedance spectroscopy (EIS) analyses. The study identified two distinct linear dynamic ranges for the detection of BPA, 0.197−2.94 and 3.5−17.72 μM. The regression equation was utilized to determine the sensitivity and limit of detection (LOD), resulting in values of 0.6 μA cm^{-2} μM^{-1} and 0.02 μM (S/N = 3), respectively. The kinetics of BPA oxidation at the polyCoRu/GCE were investigated to evaluate the heterogeneous rate constant (k), charge transfer coefficient (α), and the number of electrons transferred during the oxidation and rate-determining step. A probable electrochemical reaction mechanism has been presented for further comprehending the phenomena occurring at the electrode surface. The practical applicability of the fabricated electrode was analyzed using tap water, resulting in a high percentage of recovery ranging from 96 to 105%. Furthermore, the reproducibility and stability data demonstrated the excellent performance of polyCoRu/GCE.

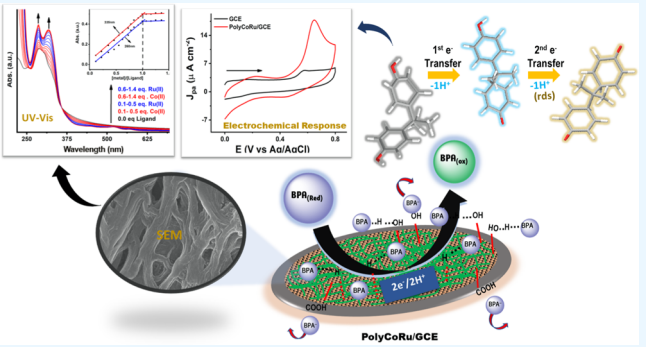

1. INTRODUCTION

Bisphenol A (BPA) is a widely used organic compound in the production of polycarbonates, epoxy resins, and plastics.[1,2] BPA is predominantly discharged into the environment via sewage treatment effluent, landfill leachate, and natural degradation of polycarbonate plastics, resulting in soil and water contamination.[3] Furthermore, owing to its unstable and lipophilic nature, BPA has the potential to migrate into food products stored in polycarbonate plastics when subjected to high temperatures.[4] BPA exhibits structural similarity to endogenous estrogen, thereby enabling its binding to the estrogen receptor, which is also targeted by estradiol.[4] Thus, by mimicking the role of estradiol, this substance functions as a conventional endocrine disruptor, potentially resulting in adverse health outcomes, such as prostate cancer, heart disease, infertility, obesity, and liver function abnormalities.[5] The deleterious effects on sexual organs can be observed even at low concentrations of BPA in parts per billion.[6] As a result of its detrimental impact, a number of industrialized nations, including the United States, China, and the European Union, have implemented bans on the utilization of BPA in plastic merchandise and packaging components.[7−9] Hence, the efficient detection and removal of BPA has become an important issue for researchers.

The development of a method that can effectively detect the presence of BPA is of utmost importance for the well-being of both human health and the environment. Such a method should possess the qualities of accuracy, speed, simplicity, and affordability. Several techniques have been devised for the detection of BPA, such as tandem gas chromatography-mass spectroscopy, high-performance liquid chromatography, capillary electrophoresis, fluorescence, chemiluminescence, and

Received: April 9, 2023
Accepted: July 13, 2023
Published: July 24, 2023

Scheme 1. (a) Preparation of Co−Ru-Based M-SMP Is Depicted Schematically and (b) Modification of the Bare GCE by a Dispersed PolyCoRu Solution

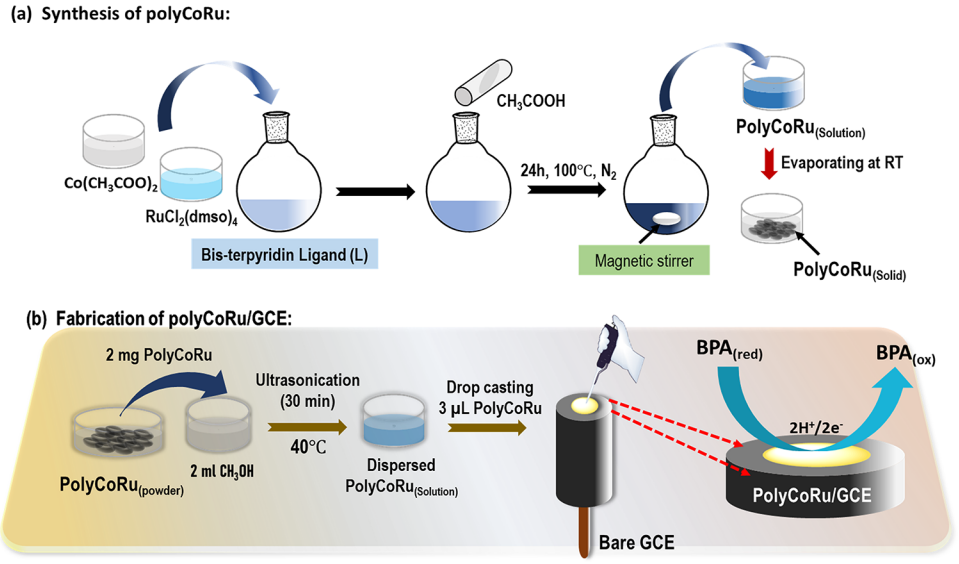

Raman scattering.[1−4,7] However, these techniques are expensive, laborious, and necessitate intricate sample preparation. In contrast, electroanalytical methods have garnered significant interest owing to their cost-effectiveness and the ease with which electrodes can be modified with minimal treatment time. Recently, electrodes that have been subjected to modifications with diverse materials have gained significant traction in the development of BPA sensors. This is primarily due to the limited selectivity of conventional electrodes. Therefore, the development of novel electrode modifiers to expedite the progress of BPA sensors has posed a formidable challenge. Ye et al. conducted a study on the concurrent detection of BPA and bisphenol S.[10] AuAgPt-PCD-GO, which comprises of porous β-cyclodextrin polymer (PCD), was developed with the aim of enhancing the bare surface of GCE. The sensor under consideration exhibited a notable capability to detect BPA at a relatively low limit of detection (LOD). The synthesis of the composite material required a multistep pathway, which prompted the need for a simpler synthesis pathway to facilitate the production of novel materials with greater ease and feasibility.

Supramolecular polymers (SMPs) are considered to be the result of noncovalent interactions between synthetic molecules, which lead to the formation of well-defined systems through a process that is both spontaneous and reversible, known as self-assembly.[10,11] The primary motivation for the production of heterometallo SMP lies in the fact that the reaction can occur spontaneously without the need for an initiator or catalyst, as the synthetic species self-assemble during the process. Metal−ligand interactions represent a type of noncovalent interaction that exhibits a wide range of thermodynamic stability and kinetic lability.[12] The orientation of monomers in polymeric chains is primarily influenced by various factors such as the nature of denticity, host−guest interactions, ligand size, organic ligand functionality, solvent systems, and pH levels.[13,14] As a result, changes in the structural properties of a polymer may have an impact on its electrical conductivity and solubility in a solvent.[15,16] The diverse field of application for metal SMPs (M-SMPs) is attributed to their varying structural properties. These applications include electrochromic displays, sensing devices, dye-sensitized solar cells, energy storage and conversion devices, and water splitting (primarily in the context of oxygen evolution reactions).[14,15,17] One of the challenges in preparing M-SMPs is to develop a design strategy that is both efficient and suitable for experimental conditions. This involves selecting the appropriate metal and organic linker and gaining an understanding of the host−guest bonding mechanism, which may involve stacking, hydrogen bonding, or coordination bonding.[13,15,18] The primary advantage of utilizing M-SMP lies in its ability to augment electroactive characteristics through coordination bonding facilitated by metal−metal interaction.[13,16−20]

To date, various metallic species, namely, Co, Cu, Ni, Au, and Zn, have been used owing to their heightened capacity to catalyze the oxidation of BPA.[21−24] The bisterpyridine ligand, [4′,4‴-(1,4-phenylene)bis(2,2′:6′,2″-terpyridine)], is widely recognized as a better option for constructing M-SMPs due to its potent chelating capabilities. This is attributed to the presence of N-heterocycles within the ligand, which exhibits a high affinity for metal binding and readily engages in $\pi-\pi^*$ interactions with metal ions.[20,25]

The present study involves the synthesis of an organometallic electrocatalyst, namely, Co(II)Ru(II)-bis terpyridine heterometallo-supramolecular polymer (HM-SMP), through a 0.5:0.5:1 complexation approach. The objective of this approach is to enhance the surface properties of glassy carbon electrode (GCE). The selection of GCE as a substrate was based on its operational convenience. The synthesized material (polyCoRu) was used as the electrode material for the electrochemical oxidation of BPA. The material synthesized through a facile one-pot method exhibited exceptional electrocatalytic performance in the oxidation of BPA at a micro level of 0.02 μM. Under optimal conditions, two linear ranges were determined to be 0.197−2.94 and 3.5−17.72 μM. The fabricated modified electrode was used to ascertain the percentage of BPA recovery in a tap water sample, with the aim of evaluating its practical utility.

https://doi.org/10.1021/acsomega.3c02206
ACS Omega 2023, 8, 28355−28366

2. EXPERIMENTAL SECTION

2.1. Materials. The entire experiment was conducted using deionized water (DI). Acetic acid (CH_3COOH) was used as a solvent in the process of polymer synthesis. In addition, dimethyl sulfoxide (DMSO), methanol (CH_3OH), acetone (CH_3COCH_3), and acetonitrile (CH_3CN) were used for various purposes. BPA ($((CH_3)_2C(C_6H_4OH)_2)$) was used as a targeting analyte for this experiment. The salts used for the selectivity analysis were ascorbic acid (AA), $AlCl_3$, $CdSO_4$, hydroquinone, $MgSO_4$, Na_2CO_3, NaCl, and $Pb(OAc)_2$. Potassium ferricyanide $[K_3Fe(CN)_6]$ in potassium chloride (KCl) was utilized as a redox probe. The ligand utilized in the polymer synthesis was 4′,4‴-(1,4-phenylene) bis(2,2′:6′,2″-terpyridine), whereas the metal salts used were cobalt acetate ($C_4H_6CoO_4$) and tetrakis (dimethyl sulfoxide) dichloro ruthenium(II) ($RuCl_2(dmso)_4$). Sodium dibasic phosphate (Na_2HPO_4) and sodium monobasic phosphate (NaH_2PO_4) were exploited to prepare a phosphate buffer solution (PBS) as a supporting electrolyte. All of the aforementioned items were procured from Sigma-Aldrich.

2.2. Preparation of Co−Ru-Based Supramolecular Polymers. Co−Ru-based heterometallo SMPs were prepared by following a facile complexation reaction strategy (Figure S1). A complexation approach was carried out by using [4′,4‴-(1.4-phenylene)bis(2,2′:6′,2″-terpyridine)] (L) as a ligand with a prominent chelating effect. L was treated with cobalt acetate and tetrakis (dimethyl sulfoxide) dichloro ruthenium-(II) salts. Acetic acid and methanol were used as solvents for the reaction. The aforementioned reaction was conducted in a 100 mL round bottom flask under N_2 pressure for 24 h at 100 °C (Scheme 1a). In this SMP synthesis, L was synthesized by following the previous report.[26] At the very end of the complexation reaction, a dark orange-colored solution appeared. A solid powder resembling closely to dark orange-colored SMP was obtained with a high percentage of yield. The molecular weight of the synthesized polymer was calculated using size exclusion chromatography−viscometry−right-angle light scattering (SEC-VISC-RALS) method and determined to be 13.1 × 10^5 Da. The average degree of polymerization was found to be 750, which was calculated from the molecular weight of the polymer, and the length of the polymer chain was measured to be 1061.85 nm. Moreover, the distance between the two metal centers was 1.1 nm, which was determined using molecular modeling (Figure S2). EDX analysis was performed to identify the presence of different elements in polyCoRu (Figure S3).

2.3. Fabrication of PolyCoRu/GCE. A uniformly dispersed clear solution of polyCoRu was deposited on the bare GCE surface via the simple drop casting method using a micropipette (Scheme 1b). For preparing a homogenous solution of polyCoRu, 2 mg of polyCoRu was subjected to sonication for a duration of 30 min in a 2 mL solution of methanol. Prior to drop casting, the GCE was carefully polished on a polishing cloth using a 0.05 μm alumina/water slurry (Buhler, Germany) until a mirror-like finish was achieved. To remove any traces of excess slurry, the polished GCE was washed several times with a rapid flow of a sufficient amount of DI. Then, the GCE was modified by drop casting 3 μL of the dispersed solution with no binding agent, followed by drying at room temperature. A volume of 3 μL of polyCoRu solution was utilized due to its low charging current and optimal analyte response.

2.4. Measurements and Instruments. Field emission scanning electron microscope (FE-SEM), FT-IR, and UV/Vis spectrophotometer were utilized for evaluation of morphological and structural properties. FE-SEM: JOEL, Model: JSM 7600 F was used for evaluating the surface morphology of the fabricated polymer along with the structural change. IR spectra were obtained using the IR tracer-100 Shimadzu in order to determine the functional groups present on the surface of the polymer. Furthermore, in order to investigate the structural characteristics and ratios of complex formation, a Shimadzu UV-1800 UV−vis spectrophotometer with a double-beam configuration was used. A three-electrode, one-compartment cell was used throughout the electrochemical experiment. GCE, or polyCoRu-modified GCE (polyCoRu/GCE), was exploited as a working electrode. Platinum wire (Pt wire) and Ag/AgCl (in saturated KCl solution (1 M)) were used as counter electrodes and reference electrodes, respectively. CV and EIS were analyzed for bare and modified electrode surface characterization. All electrochemical experiments were carried out using a single potentiostat CH Instrument workstation (CHI 660E). For sonication purposes, an ultrasonicator, sonic 360, was used.

3. RESULTS AND DISCUSSION

3.1. Structural Analysis of PolyCoRu Polymer. The linear structure of polyCoRu was confirmed through the utilization of UV−vis spectrophotometric titration (Figure 1a).

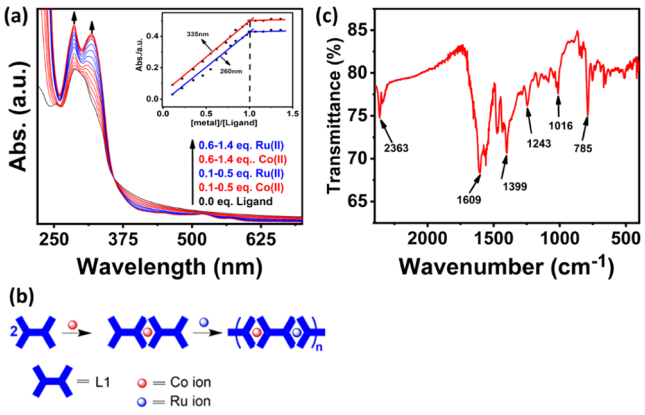

Figure 1. (a) UV−vis spectrophotometric analysis, using the solvents (CH_3CN and CH_3COOH, $c = 5 \times 10^{-4}$ M) to an L solution (solvent: MeOH, 1.0×10^{-5} M, l = 1 cm) at 25 °C. The absorbance changes at wavelengths of 260 and 335 nm are displayed in the inset as a function of the total number of metal ions [(Co + Ru)]/[L]. (b) Simple complexation scheme predicted based on UV−vis spectra. (c) FT-IR spectrum for polyCoRu material.

An outer sphere coordination reaction between bis-terpyridine ligand (L) and metal ions (Co(II) and Ru(II)) was observed due to metal-to-ligand charge transfer (MLCT) and/or ligand-to-metal charge transfer (LMCT) reactions through the formation of a bridging compound. An upward trend in absorption was observed at 335 nm upon the addition of 0.5 equiv of Ru(II) salt to the L solution in the spectrum. The observed phenomenon can be ascribed to the intricate bonding between Co(II) and the terpyridine moiety of L, which is depicted in Figure 1a (inset) and is represented by the blue spectra. Subsequently, a further MLCT absorption was observed at a wavelength of 260 nm subsequent to the introduction of a solution of Ru(II) salt into the solution

https://doi.org/10.1021/acsomega.3c02206
ACS Omega 2023, 8, 28355−28366

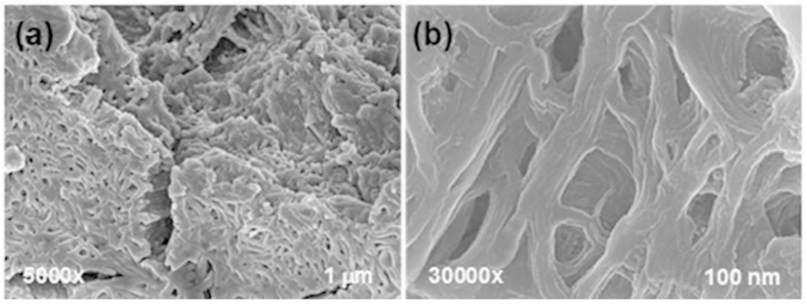

Figure 2. (a) SEM images and (b) magnified SEM images for polyCoRu material.

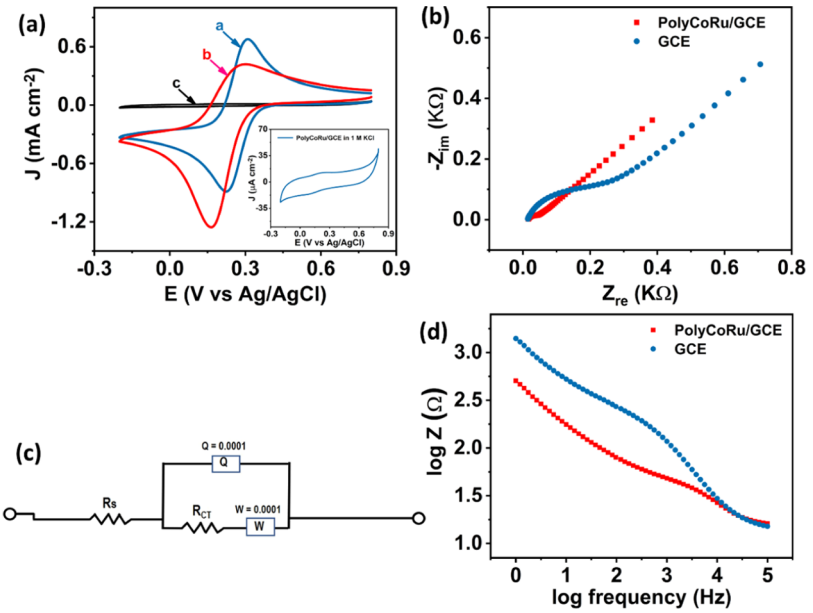

Figure 3. (a) CVs for GCE in 5 mM $K_3[Fe(CN_6)]$, polyCoRu/GCE in 5 mM $K_3[Fe(CN_6)]$, and polyCoRu/GCE in 1 M KCl solution indicated by a, b, and c, respectively, CV of polyCoRu/GCE in 1 M KCl (inset). (b) Nyquist plots for the bare GCE and the polyCoRu/GCE in 5 mM $K_3Fe(CN)_6$ solution. (c) Corresponding Randle circuit from fitting the Nyquist plot; here, R_s is the solution resistance, R_{CT} is the charge transfer resistance, W is the Warburg resistance, and Q is the constant phase element. (d) Bode plot to support the Nyquist plot.

comprising of L and Co(II) ions at a molar ratio of 1:0.5. The absorption peak exhibited an increase in relation to [Co(II)/L] upon the addition of up to 0.5 equiv of Ru(II), suggesting the initial formation of a 1:2 complex between Co(II) and L, followed by the formation of a 1:1 complex between Co(II) ion and Ru(II) complex. Remarkably, the introduction of additional Ru(II) and Co(II) salts into the solution did not result in any discernible augmentation of the absorption peak. This observation strongly implies the verification of the formation of a complex involving L/Co(II)/Ru(II) in a ratio of 1:0.5:0.5. The UV−vis spectra were utilized to predict a basic complexation scheme, which is illustrated in Figure 1b. The assessment of characteristic functional groups was conducted via FT-IR analysis, as depicted in Figure 1c. The terpyridine moiety exhibited characteristic stretching bands in the fingerprint region spanning from 1600 to 1450 cm^{-1}, corresponding to (C═O), (C═C), and (C−H) stretching vibrations.[27,28] The appearance of the medium (O−H) bending vibration within the range of 1440−1330 cm^{-1} may be attributed to the presence of carboxylic and alcoholic hydroxyl groups. Stretching bands of (C−N) and (C−C) vibrations were observed within the spectral range of 1250−1000 cm^{-1}. The presence of a nitrogen-containing ligand in the polymer is indicated by the (C−N) stretching band observed in the FT-IR spectrum. Moreover, the medium bending vibration of the C═C bond was observed within the spectral range of 840−790 cm^{-1}.[29]

Morphological features of the polyCoRu polymer were investigated by using SEM. Figure 2a,b shows the SEM images at various magnifications. The linear chain structure with network connections of the polymer chain is clearly visible in different magnified SEM images. These network structures are mainly responsible for the interaction between ligands and metal ions of different chains. The linear arrangement of polyCoRu exhibited similarity with the results obtained from UV−vis spectrophotometric analysis. Furthermore, the verification of the existence of diverse elements was ascertained through the utilization of EDX, as depicted in Figure S3, wherein the percentage quantities of distinct atoms are presented in the inset.

3.2. Characterization of PolyCoRu/GCE through CV and EIS Techniques. The electrochemical behavior of Co- and Ru-based supramolecular polymers as electrode materials was assessed using $K_3[Fe(CN)_6]$ solution as a redox probe. CV as well as EIS techniques were used to analyze the changes in redox reaction in $K_3[Fe(CN)_6]$ solution at polyCoRu-modified GCE (illustrated in Figure 3a,b). Figure 3a represents the CV plot for a 5 mM $K_3[Fe(CN)_6]$ solution prepared in 1 M KCl

https://doi.org/10.1021/acsomega.3c02206
ACS Omega 2023, 8, 28355−28366

using both GCE and polyCoRu/GCE electrodes. Peak-to-peak separation (ΔE_p) for the bare electrode was found to be 71 mV (0.269/0.340 V), which was almost close to the ideal value (ΔE_p = 59 mV), confirming the reversible manner according to the Nernst equation. Whereas for the modified electrode, ΔE_p was found to be 137 mV (0.165/0.302 V), which indicates the quasi-reversible electrochemical charge transfer at the electrode/electrolyte surface. The ratio of anodic to cathodic peak current (I_{pa}/I_{pc}) was analyzed to identify the reversibility at polyCoRu/GCE. The bare GCE ((I_{pa}/I_{pc}) ~0.99) exhibited complete reversible behavior, whereas the polyCoRu/GCE ((I_{pa}/I_{pc}) = 0.4) showed quasi reversibility. The Fe(III)/Fe(II) process exhibited reduction peak currents of 52.8 and 84.46 μA for the bare and modified electrodes, respectively. This indicates that the polyCoRu/GCE demonstrated a peak current 1.6 times higher than that of the bare GCE. The reason for enhanced reduction peak response was confirmed through the derivation of the effective surface area (ESA) of both electrode systems. According to the Randles−Sevcik equation, ESA can be calculated as follows: $I_p = 2.69 \times 10^5 \sqrt[3]{n} A_{eff} \sqrt{D} C_0 \sqrt{\nu}$, where I_p is the peak current, ν is the scan rate, and C_0 represents the bulk concentration of an analytic solution (5 mM $K_3[Fe(CN)_6]$ in 1 M KCl). Moreover, n is the number of electrons transferred during the redox reaction and D is the diffusion coefficient (7.6×10^{-6} cm^2 s^{-1} for $K_3[Fe(CN)_6]$ redox probe). Regarding the reduction peak, the estimated ESAs for both bare GCE and polyCoRu/GCE were 0.064 and 0.082 cm^2, respectively. Thus, the modified electrode showed an enhanced current response for the reduction of Fe(III) species to Fe(II) compared to the bare GCE, which implies electrochemically improved surface properties in the case of polyCoRu/GCE. The reason for the higher cathodic response (electrochemical conversion of Fe(III) to Fe(II)) of polyCoRu/GCE is due to the attraction between positively charged metal ions of polyCoRu and negatively charged $[Fe(CN)_6]^{3-}$. The suppression of the anodic peak current of polyCoRu/GCE is most likely due to the coordination bond formation of Fe(II) with the ligand.

The EIS plot shown in Figure 3b was performed in the 1 Hz to 100 kHz frequency range to represent the electron transfer abilities of both electrode systems for a similar redox probe. Formal potentials for both the bare and modified electrodes were set at 0.304 and 0.234 V, respectively. The charge transfer resistance (R_{CT}) is represented by the semicircle portion of the Nyquist plot at higher frequencies, and the electron transfer is represented by the linear portion at lower frequencies corresponding to diffusion-controlled phenomena.[30] The small semicircle part of the modified electrode (~100 Ω) compared to the bare GCE (~320 Ω) is likely to enhance electron transfer at the interface. This observation completely upholds the results obtained from the CV analysis. Figure 3c corresponds to the simulated Randle circuit for the fitted Nyquist plot. Moreover, the corresponding Bode plot shown in Figure 3d, showing the change of impedance with frequency, was also investigated for further analysis of EIS data. The R_{CT} corresponding to the modified electrode leads to a lower value compared to the bare electrode. This further supports the unavailability of electron transfer for the reverse oxidation half-cell reaction.

3.3. Electrochemical Behavior of PolyCoRu/GCE toward BPA Detection. The feasibility of electron transfer of BPA has been examined through the implementation of cyclic voltammetry (CV) technique in a solution of 3 μM BPA in 0.1 M PBS, utilizing both polyCoRu/GCE and GCE. CV responses for blank (0.1 M PBS) and 3 μM BPA prepared in 0.1 M PBS at GCE and a modified GCE are illustrated in Figure 4. The blank solution yielded no signal at both the bare

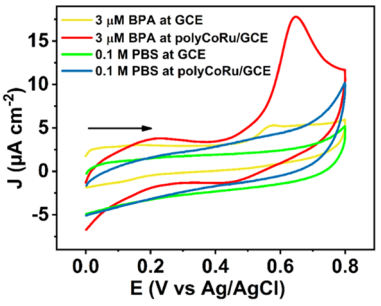

Figure 4. CV plot for polished GCE and polyCoRu/GCE for blank 0.1 M PBS and 3 μM BPA in 0.1 M PBS solution.

GCE and modified electrode. The polyCoRu/GCE exhibited a distinct and improved current signal at ~0.65 V, in contrast to the bare GCE which produced a significantly lower and less defined current response at 0.56 V when exposed to the identical BPA solution. The increased peak current observed in the polyCoRu/GCE electrode indicates the potential suitability of this electrode for the oxidation of BPA, when compared to the unmodified electrode. A lower current response was observed during the reverse CV scan at the modified electrode within the potential range of 0.4−0.5 V. Proton adsorption on the surface of the polymer may be the cause of this broad reduction peak. This occurred most likely owing to the release of protons at the inner Helmholtz layer (IHL) during the oxidation of BPA. The investigation revealed that the maximum current for the oxidation of BPA on polyCoRu/GCE was 0.74×10^{-6} A, a value that was ~4 times greater than that observed on the unmodified GCE, which was 0.18×10^{-6} A. The electrocatalytic activity of chemically synthesized HM-SMP toward BPA oxidation is excellent, likely due to the enhanced current response at polyCoRu/GCE, which is expected to have a larger surface area compared to bare ones.

3.4. Evaluation of Electrode Parameters. Quantitative analysis of BPA at various concentrations was performed using DPV for the purpose of sensitive detection. The DPV plot for BPA is depicted in Figure 5a, covering a concentration range of ~0.197 to 17.72 μM in 0.1 M PBS with a pH of 7. A positive correlation was observed between the concentration of BPA and the current signal, indicating an upward trend. However, at higher concentrations, peak current shifts toward more positive potential. This phenomenon is most likely attributed to the deposition of more BPA at the modified surface which causes more potential for oxidation. Two linear fits were obtained for the concentration range depicted in Figure 5b when plotting the anodic peak current density against the concentration of BPA, as evidenced by the calibration plot. The regression equation for the concentration range of 0.197−2.94 μM was $J_{pa} = 6.94 \times 10^{-7} + 5.99 \times 10^{-7} \times [BPA]$ (μM) with a regression coefficient value of 0.99. The second linear fit was obtained for the concentration range of 3.5−17.72 μM. In this case, the regression equation was $J_{pa} = 2.33 \times 10^{-6} + 3.72 \times 10^{-8} \times [BPA]$ (R^2 = 0.99). The obtained regression equations indicate that the sensitivity value for the concentration range of 0.197−

https://doi.org/10.1021/acsomega.3c02206
ACS Omega 2023, 8, 28355−28366

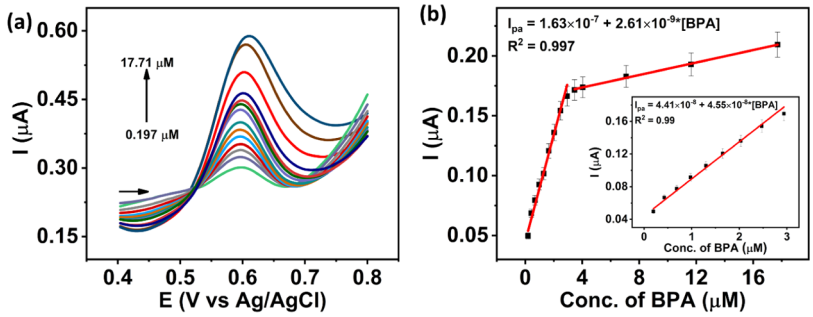

Figure 5. (a) DPV plots for concentration variation in the following order: 0.197, 0.43, 0.69, 0.98, 1.3, 1.65, 2.031, 2.471, 2.94, 3.461, 4.039, 7.08, 11.64, and 17.71 μM of BPA in 0.1 M PBS (pH 7.0). (b) Corresponding plot of peak current (I_{pa}) vs concentration of BPA.

Table 1. Linear Range and LOD of the PolyCoRu/GCE for BPA Oxidation are Compared with Previously Reported Sensors[a]

electrode	method	linear range (μM)	LOD (μM)	reference
polyCoRu/GCE	DPV	0.197−2.94	0.02	this work
		3.5−17.72		
PANI_AuNPs/GCE	DPV	0.003−0.064	0.0004	31
		0.075−45.69		
PAMAM-AuNPs-SF/GCE	CV	0.001−1.33	0.0005	32
ITO electrode	DPV	0.5−50	0.4	33
CS-Fe_3O_4/GCE	CV	0.05−30	0.008	34
PGA/MWCNT-NH_2/GCE	CV	0.1−10	0.02	35
CuPc/MWCNT-COOH/PGE	DPV	0.1−27.5	0.0189	36
TM-β-CD-Gr/PtNPs/GCE	CV	0.05−80	0.015	37
PtPd-CP_5@RGO/GCE	DPV	0.01−50	0.0033	38
		50−1000		
MIPN/GCE	DPV	0.02−1.0	0.008	39
NH_2-MIL-125/RGO/GCE	CV	2−200	0.7966	40
N-G/M-GCE	DPV	0.05−20	0.08	41

[a]Note: PANI_AuNPs/GCE: polyaniline and gold nanoparticles/GCE; PAMAM-AuNPs-SF/GCE: glassy carbon electrode modified with gold nanoparticles, silk fibroin, and PAMAM dendrimers; ITO: indium tin oxide; CS-Fe_3O_4: chitosan-Fe_3O_4; PGA/MWCNT-NH_2: polyglutamate acid and amino-functionalized carbon nanotube nanocomposite modified glassy carbon electrodes; CuPc/MWCNT-COOH/PGE: pencil graphite electrode modified by adsorption of MWCNT-COOH and copper(II) phthalocyanine; TM-β-CD-Gr/PtNPs: graphene/platinum nanoparticles functionalized with heptakis-(2,3,6-tri-*O*-methyl)-β-cyclodextrin; MIPN: molecularly imprinted polymer nanocomposite; NH_2-MIL-125/RGO: amine functionalized metal−organic framework/reduced graphene oxide; N-G/M-GCE: nitrogen-doped reduced graphene oxide and melamine-modified GCE.

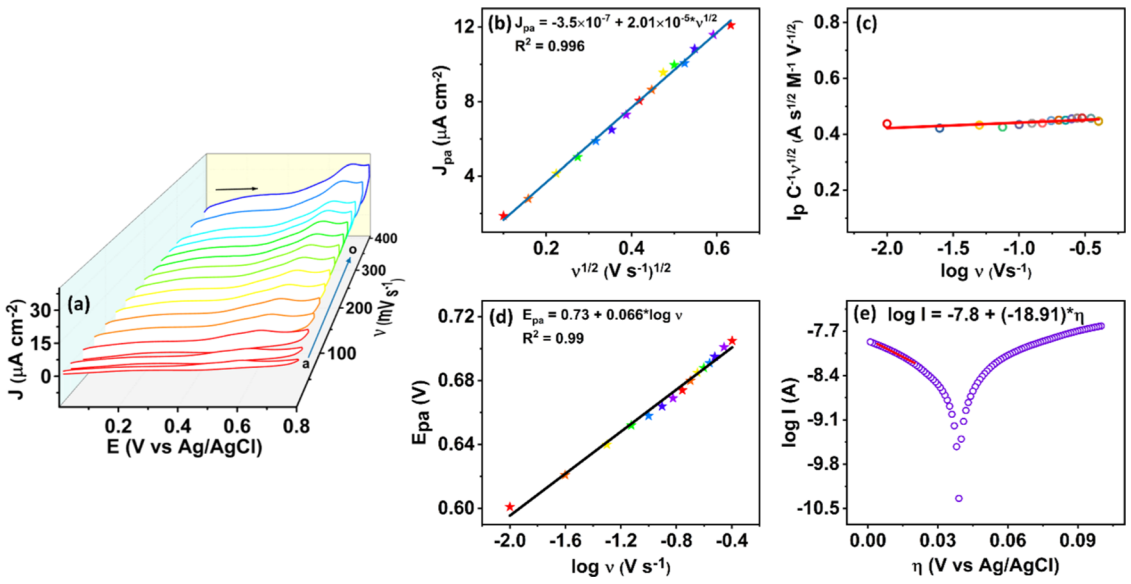

Figure 6. Effect of scan rate on 3 μM BPA oxidation at polyCoRu/GCE. (a) CV curves for different scan rates are as follows: (a−o) 10, 25, 50, 75, 100, 125, 150, 175, 200, 225, 250, 275, 300, 350, and 400 mV s^{-1}. The relevant curves are (b) J_{pa} vs $\nu^{1/2}$, (c) I_p C^{-1} $\nu^{-1/2}$ vs log ν, and (d) E_{pa} vs log ν. (e) Tafel plot analysis was performed at a scan rate of 5 mV s^{-1}.

https://doi.org/10.1021/acsomega.3c02206
ACS Omega 2023, 8, 28355−28366

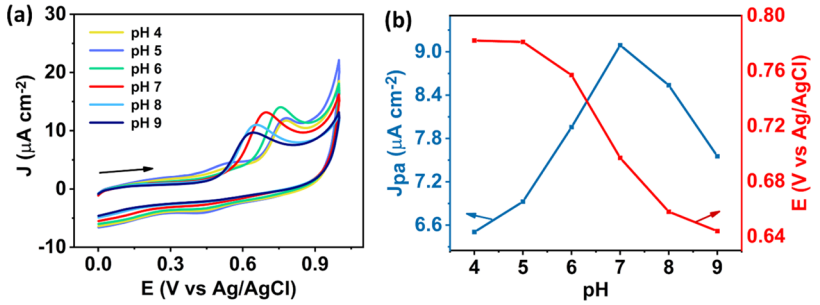

Figure 7. (a) CV curves for different pH values in the range of 4−9 for a 3 μM BPA solution in 0.1 M PBS at polyCoRu/GCE; (b) plots to show the relationship [between pH and peak current density and potential as well (baseline corrected values from CVs unless otherwise mentioned)].

2.94 μM was 0.6 μA cm to 2 μM^{-1}. The present analysis confirms that the modified electrode exhibits reduced sensitivity with increasing concentration. LOD was determined to be 0.02 μM using the formula of LOD = 3.3 × SD/S. Similarly, the limit of quantification (LOQ) was found to be 0.061 μM using LOQ = 10 × SD/S, where SD stands for standard deviation and S represents the slope of the regression equation. The proposed polyCoRu/GCE has demonstrated a promising BPA sensing capability when compared to other electrochemical BPA sensors regarding quite straightforward electrode preparation and cheaper electrode materials. Some electrochemical parameters of polyCoRu/GCE and previously reported electrodes for electrochemical oxidation of BPA are represented in Table 1.

3.5. Investigation of the Kinetics of Electron Transfer in BPA Oxidation at PolyCoRu/GCE. The effect of various scan rates was analyzed for electrochemical oxidation of 3 μM BPA in 0.1 M PBS using the CV technique to evaluate the kinetics of the heterogeneous electron transfer process at the modified electrode. The kinetics at the interface were investigated by determining the electron transfer coefficient (α), heterogeneous charge transfer constant (k), and effective electrode surface area (A_{eff}) using the classical Butler−Volmer theory. These are typical kinetic parameters used in such analyses. The CV plots (Figure 6a) indicate that there was an augmentation in the current signal as the scan rate was elevated from 10 to 400 mV s^{-1}. Figure 6b shows a linear relationship between anodic peak current density and the square root of the scan rate. The regression equation $J_{pa} = -3.5 \times 10^{-7} + 2.01 \times 10^{-5} \times \nu^{1/2}$ with a regression coefficient of 0.996 exhibited excellent linear fit between these two terms. Thus, after analyzing the calibration plot, it has been confirmed that the electron transfer during BPA oxidation at the interface is controlled by diffusion.

According to the Randles−Sevcik equation, the constant ratio of I_p to $C\nu^{1/2}$ for an ideal irreversible process is logarithmically related to the scan rate.[42] The relationship between peak current and scan rate was examined by plotting $I_pC^{-1}\nu^{-1/2}$ vs $\log \nu$ plot (Figure 6c) in order to confirm the findings. Moreover, a linear plot was obtained between E_{pa} vs $\log \nu$ (Figure 6d). Thus, the following formula is applicable to a typical irreversible system

$$E_p = Y + \frac{2.303RT}{2(1-\alpha)n_\alpha F} \log \nu \quad (1)$$

Here, the symbols R, T, and F represent the universal gas constant, absolute temperature, and Faraday constant, respectively. Moreover, n_α is the total number of electrons transferred during the rate-determining step (RDS), α is the charge transfer coefficient, and the value of α is $(0 < \alpha < 1)$, whether the transition state is reactant (<1) or product (~1).[31] The electrochemical feasibility of BPA oxidation at polyCoRu/GCE was demonstrated by utilizing the slope of eq 1, resulting in the determination of a value of α as 0.552.

The Y-intercept of eq 1 could be expressed as follows to evaluate heterogeneous rate constant (k) through the consideration of E vs $\log \nu$ plot

$$Y = E^{0'} + \frac{RT}{(1-\alpha)n_\alpha F} \times \left\{0.78 + \frac{2.3}{2} \log\left[\frac{(1-\alpha)n_\alpha FD}{K^2RT}\right]\right\} \quad (2)$$

where $E^{0'}$ is the standard electrode potential of the BPA oxidation, which is calculated from the Tafel plot, k is the heterogeneous rate constant relating to the charge transfer process, and D is the diffusion coefficient (5.83×10^{-6} cm^2 s^{-1}).

The effective surface area of polyCoRu/GCE has been calculated through the utilization of the Randles−Sevcik equation (as follows), which is suitable for the analysis of irreversible electrochemical processes

$$I_{pa} = 2.99 \times 10^5\, n[(1-\alpha)n_\alpha]^{1/2} C_0 A_{eff} D^{1/2} \nu^{1/2} \quad (3)$$

The slope of J_{pa} vs $\nu^{1/2}$ plot can be used to evaluate A_{eff} by using eq 3 and was found to be ~1.01 cm^2 (for n = 2 and D = 5.83×10^{-6} cm^2 s^{-1})[31] for polyCoRu/GCE during BPA oxidation. This enhanced surface area of the modified electrode provided more active sites for BPA oxidation which in turn facilitated electron transfer to give a large current signal.

The Tafel plot was analyzed in order to determine the total quantity of electrons (n) that participate in the process of BPA oxidation. The Tafel plot, which displays the logarithm of the current ($\log I$) against the overpotential (η), can exhibit a linear relationship within a particular range of overpotentials (η), contingent upon the number of electrons involved. By examining the Tafel plot obtained at a scan rate of 5 mV/s, featuring both oxidation and reduction waves as illustrated in Figure 6e, a linear region was identified at a higher potential during the oxidation process. The linearity observed in this region can be adequately explained by the following regression equation

$$\log I = -7.8 + (-18.91) \times \eta \quad (4)$$

Tafel slope is known as the slope of eq 4 and can be expressed as follows

https://doi.org/10.1021/acsomega.3c02206
ACS Omega 2023, 8, 28355−28366

Scheme 2. Plausible Electron Transfer Reaction Mechanism at PolyCoRu/GCE for Irreversible BPA Oxidation

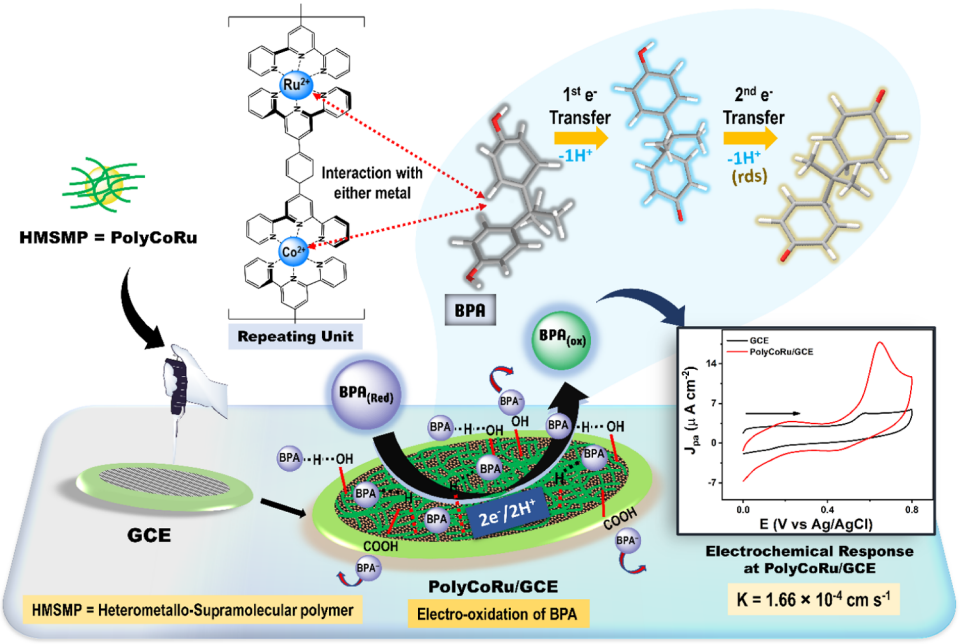

$$\frac{1}{b} = \frac{n\alpha F}{2.303RT} \quad (5)$$

The slope value of the Tafel plot was obtained as 18.91. Upon solving eq 5, it was determined that the total quantity of electrons transferred during the oxidation of BPA was two. This suggests that the oxidation of BPA takes place in two distinct stages, with the transfer of two electrons occurring consecutively. The heterogeneous rate constant (k) was determined as 1.66×10^{-4} cm s^{-1} (for $E^{0\prime}$ = 0.45 V) by solving eq 2. This value is comparable to the BPA sensor reported in previous studies.[31]

The effect of pH on peak current during oxidation of BPA was investigated to understand the effect of proton concentration during oxidation. Figure 7a illustrates that at polyCoRu/GCE, the negative potential has induced a shift in the redox peak current for 3 μM BPA solution, with the pH of the supporting electrolyte being varied. The phenomenon of peak current shifting is attributed to the protonic effect in the presence of BPA oxidation. The analysis was conducted utilizing PBS as the supporting electrolyte within the pH range spanning from 4.0 to 9.0. At very low pH, surface fouling due to material degradation might hinder BPA oxidation, which in turn leads to a decreased peak current.[31] The peak currents exhibit an upward trend within the pH range of 4.0−7.0. An increased current density (J_{pa}) has been achieved for solution pH values up to 7.0. Upon further increase of the pH of the solutions beyond 7.0, a decreasing trend in peak current was observed until a pH of 9.0. The observed phenomenon can be ascribed to the generation of phenolic oxide anion under alkaline conditions.[31,32] Based on the characterization of the modified surface using a redox probe, it can be inferred that the surface may possess negatively charged functional groups. These groups are likely to exhibit a repulsive effect toward the phenolate anionic form of BPA at a pH greater than 7. The reduction in peak current at higher pH levels may be attributed to the hindrance of the BPA approach to the interface caused by the presence of phenolate forms. As pH 7.0 exhibited higher sensitivity toward BPA oxidation at polyCoRu/GCE, entire electrochemical studies were done under pH 7.0 unless stated otherwise. The observed shift of the anodic peak toward a more negative potential with an increase in pH from 4.0 to 9.0 (Figure 7b) provides confirmation of the involvement of an equivalent proton transfer during the oxidation of BPA at the electrode/electrolyte interface.

3.6. Probable Reaction Mechanism toward BPA Oxidation. To elucidate the probable electrochemical oxidation of BPA on the surface of an HM-SMP-coated GCE, a tentative reaction mechanism involving the transfer of two electrons through either (a) direct coordination reaction through metal ions or (b) indirect electron transfer through MLCT or ligand-to-ligand charge transfer (LLCT) has been considered.[14,29,43] Both molecular interactions and kinetic studies are equally significant in determining the number of electron transfer pathways and the electrons involved in RDS. BPA molecules in the sample solution can adsorb onto the modified electrode surface through noncovalent interactions, such as hydrogen bonding, $\pi-\pi$ stacking, or electrostatic interactions. The utilization of SMP provides a favorable environment for the adsorption of BPA, thereby enhancing the sensitivity and selectivity of the electrode toward BPA detection.[31] Hydrogen bonding may facilitate the oxidation of BPA at the interface. Moreover, pH variation analysis was used to assess proton dependency on BPA oxidation. The irreversibility of BPA oxidation was confirmed from the analysis of plot $I_pC^{-1}\nu^{-1/2}$ vs $\log \nu$. The possible electrode mechanism is illustrated in Scheme 2.

The separation of opposite charge-carrying species may result in the formation of an electrochemical double layer (ECDL). This hypothesis is based on the CV analysis performed in blank PBS with polyCoRu/GCE, which yielded an almost rectangular-shaped region. The electrocatalytic property of two heterometals containing multidentate ligand was also represented in the CV experiment. The facile transfer of electrons observed at the surface of the HM-SMP may be due to the breakage of coordination bonds between the metal and ligand, thereby creating the requisite coordination sites for

https://doi.org/10.1021/acsomega.3c02206
ACS Omega 2023, 8, 28355−28366

oxidation to occur.[29] Probable routes of BPA oxidation on the modified electrode surface can be represented as follows[29]

$$\mathrm{Co(II)LRu(II)} \rightarrow \mathrm{Co(III)LRu(II)} + e^-$$

$$\mathrm{Co(III)LRu(II)} + (\mathrm{CH_3})_2\mathrm{C}(\mathrm{C_6H_4OH})_2 \rightarrow \mathrm{Co(II)LRu(II)} + (\mathrm{CH_3})_2\mathrm{C}(\mathrm{OC_6H_4OH})$$

[1st e^- transfer]

$$\mathrm{Co(II)LRu(II)} + (\mathrm{CH_3})_2\mathrm{C}(\mathrm{OC_6H_4OH})] + \mathrm{H_2O} \rightarrow \mathrm{Co(II)LRu(II)}\ (\mathrm{CH_3})_2\mathrm{C}(\mathrm{OC_6H_4O}) + 2\mathrm{H^+}$$

[2nd e^- transfer]

This equation illustrates the process of oxidation of BPA, wherein BPA undergoes a reaction with an electron (e^-) leading to the formation of a monoquinone derivative of BPA ($(CH_3)_2C(OC_6H_4OH)$). In this surface reaction, the redox-active centers within the ruthenium and cobalt-based supramolecular polymers act as electron transfer mediators, facilitating the transfer of electrons from BPA to the electrode surface. The resulting derivative species can further undergo subsequent reactions to give a diquinone derivative of BPA ($(CH_3)_2C(OC_6H_4O)$). The Bockris–Reddy formulation (eq 6) was used to support the two-electron process evaluated from the Tafel plot and to understand the intricate multistep electron transfer involved in the oxidation of BPA.[44]

$$\alpha_a = \frac{n_b}{\nu} + n_r\beta \tag{6}$$

wherein α_a is the multistep electron transfer coefficient, n_b refers to the number of electrons transferred prior to the RDS, ν denotes the total number of RDSs involved in the electrochemical reaction, n_r represents the number of electrons transferred during the RDS, and β is the symmetry factor. Considering the values, n_b = 1, n_r = 1, ν = 1, and β = 0.28. Upon substitution of the aforementioned values into eq 6, α_a was calculated to be 21.6 mV^{-1} dec. This value bears resemblance to the experimental Tafel slope value (18.91 mV^{-1} dec) obtained using eq 5. The aforementioned observation serves as evidence that RDS constitutes the second step of electron transfer, whereby solely one electron transfer occurs at the interface between the electrode and electrolyte.[45] The possible electrode mechanism is illustrated in Scheme 2.

3.7. Reproducibility and Stability Test. The experimental stability of polyCoRu/GCE toward BPA was assessed through the utilization of amperometric technique. Figure 8a demonstrates the exceptional stability of polyCoRu/GCE over a period of 2000 s, as observed in both 0.1 M PBS and 5 μM BPA solution. In addition, the reproducibility of the experiment was evaluated by introducing modifications to five distinct GCEs utilizing polyCoRu supramolecular polymer. In order to assess reproducibility, solutions of BPA at concentrations of 5 and 3 μM were used to measure peak currents using the DPV technique. Figure 8b illustrates the peak currents for five newly modified electrodes. RSD (%) values were calculated for both 5 and 3 μM BPA solutions and found to be 4.78 and 4.48%, respectively. The results indicate that the modified electrode displays exceptional stability and reproducibility, as evidenced by the relative standard deviations being less than 5. This, in turn, confirms the practical applicability of the modified electrode.

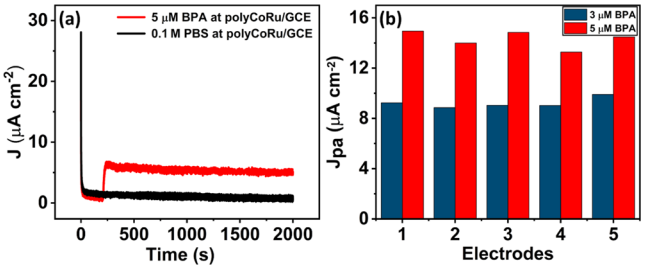

Figure 8. (a) i–t responses of 0.1 M PBS and 5 μM BPA at polyCoRu/GCE. (b) Peak current responses, measured at various BPA concentrations for four different GCEs.

3.8. Interference Test. The attainment of precise quantitative outcomes has been realized through the achievement of selectivity of the prepared polyCoRu with regard to the detection of BPA, while simultaneously analyzing commonly occurring species in real samples that may act as interfering agents. In order to evaluate the efficacy of our modified electrode, we have examined the impact of nine notable interfering agents, namely, ascorbic acid (AA), aluminum chloride ($AlCl_3$), cadmium sulfate ($CdSO_4$), hydroquinone (HQ), potassium bromide (KBr), magnesium sulfate ($MgSO_4$), sodium carbonate (Na_2CO_3), sodium chloride (NaCl), and lead acetate ($Pb(OAc)_2$). The analysis was conducted using 0.1 M PBS (pH = 7) as the supporting electrolyte. The DPV technique was utilized to observe the response toward the interfering species, in conjunction with a 5 μM BPA solution. The electrode has exhibited a noteworthy reaction to BPA, as depicted in Figure 9. For each interference, we utilized a concentration of ~10 times higher (~50 μM) than that of the BPA solutions. The species under investigation did not exhibit any discernible current responses, whereas a distinct peak current response was observed in the potential range of 0.4–0.8 V upon exposure to a 5 μM BPA solution. The present analysis provides confirmation that the polyCoRu/GCE exhibits exceptional selectivity with respect to BPA.

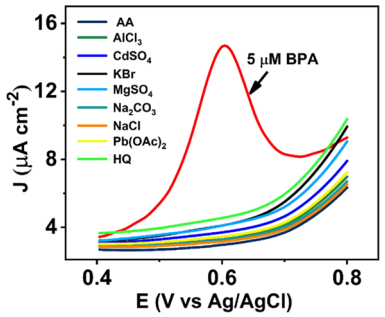

Figure 9. DPV plots for different interfering species, (i) AA (ascorbic acid), (ii) $AlCl_3$, (iii) $CdSO_4$, (iv) HQ (hydroquinone), (v) KBr, (vi) $MgSO_4$, (vii) Na_2CO_3, (viii) NaCl, and (ix) $Pb(OAc)_2$ to test the selectivity of polyCoRu/GCE toward BPA sensation (5 μM BPA in 0.1 M PBS).

3.9. Analyses of Real Samples. The practical applicability of the fabricated polyCoRu/GCE was analyzed to detect BPA in tap water samples using the CV technique. In this real-sample analysis, 0.5, 0.75, 1, and 5 μM BPA solutions were prepared both in DI water and tap water using the standard

https://doi.org/10.1021/acsomega.3c02206
ACS Omega 2023, 8, 28355–28366

addition method. The recovery of concentrations was obtained via comparison with standard BPA samples in DI water. Table 2 demonstrates the obtained results. The study determined

Table 2. Relative Standard Deviation (RSD) and Recovery Values of BPA from a Sample of Tap Water Using PolyCoRu/GCE

tap water sample no.	added BPA (μM)	found BPA (μM)	RSD (%)	recovery (%)
1	0.5	0.489	1.63	97.72
2	0.75	0.744	0.57	99.19
3	1	1.02	1.27	101.81
4	5	5.16	2.25	103.23

that the relative standard deviation (RSD) fell within the range of 0.57−2.25%, a value that is less than 3%. This finding indicates that the RSD is suitable for practical applications. Moreover, the practical applicability of the polyCoRu/GCE that was fabricated was confirmed by the high recovery values falling within the range of 97.72−103.23%.

4. CONCLUSIONS

In this study, a highly efficient sensor for detecting BPA was presented. The sensor used a polyCoRu-based supramolecular polymer as a modifier, which was synthesized through a straightforward physicochemical pathway that eliminated the need for multiple steps such as separation and purification. The size exclusion chromatography (SEC) technique was used to determine the molecular weight of polyCoRu, which was found to be 13.1×10^5 Da. Additionally, the complexation between metal ions and ligands in a 0.5:0.5:1 ratio was verified through UV−vis spectrophotometric results. The CV analysis demonstrated the effectiveness of fabricated electrodes toward BPA oxidation with high sensitivity compared to bare GCE electrodes. In this study, we conducted an analysis of the electron count using kinetic investigation through Tafel plot analysis. The findings indicate that the kinetics of oxidation is a process that entails the transfer of two electrons. The modified electrode showed two linear ranges from 0.197 to 2.94 μM (sensitivity = 0.6 μA cm^{-2} μM^{-1}) and 3.5 to 17.72 μM. LOD was calculated to be 0.02 μM. The polyCoRu/GCE was used for the purpose of detecting tap water containing BPA, with the aim of evaluating the real-time analysis capabilities of the sensor. Furthermore, the electrocatalytic efficacy of polyCoRu was demonstrated through stability and reproducibility assessments. The novel polyCoRu-modified GCE fabricated in this study exhibits potential as a sensing device for detecting the presence of the highly toxic and health-hazardous compound, BPA.

■ ASSOCIATED CONTENT

Supporting Information

The Supporting Information is available free of charge at https://pubs.acs.org/doi/10.1021/acsomega.3c02206.

Synthesis of polyCoRu, Co−Ru distance in polyCoRu, and EDX analysis for elemental investigations (PDF)

■ AUTHOR INFORMATION

Corresponding Authors

Md. Delwar Hossain − *Department of Chemistry, Jagannath University, Dhaka 1100, Bangladesh*; Phone: +880 2 226638838; Email: delwar0171038512@yahoo.com; Fax: +880 2 7113713

A. J. Saleh Ahammad − *Department of Chemistry, Jagannath University, Dhaka 1100, Bangladesh*; orcid.org/0000-0001-7568-5268; Phone: +880 2 226638838; Email: ajsahammad@chem.jnu.ac.bd; Fax: +880 2 7113713

Authors

Abdul Awal − *Department of Chemistry, Jagannath University, Dhaka 1100, Bangladesh*

Santa Islam − *Department of Chemistry, Jagannath University, Dhaka 1100, Bangladesh*

Tamanna Islam − *Environmental Science & Engineering Program, University of Texas at El Paso, El Paso, Texas 79968, United States*; orcid.org/0000-0001-9067-4372

Md. Mahedi Hasan − *Environmental Science & Engineering Program, University of Texas at El Paso, El Paso, Texas 79968, United States*; orcid.org/0000-0001-7683-4544

S. M. Abu Nayem − *Department of Chemistry, Jagannath University, Dhaka 1100, Bangladesh*

Md. Mahmudul Haque James − *Department of Chemistry, Jagannath University, Dhaka 1100, Bangladesh*

Complete contact information is available at: https://pubs.acs.org/10.1021/acsomega.3c02206

Author Contributions

[§]A.A. and S.I. contributed equally to this work

Notes

The authors declare no competing financial interest.

■ ACKNOWLEDGMENTS

This work was supported by The World Academy of Sciences (TWAS) research grant program (Ref 21-311 RG/CHE/AS_G-FR3240319511) and the Ministry of Science and Technology, Bangladesh.

■ REFERENCES

(1) Sambe, H.; Hoshina, K.; Hosoya, K.; Haginaka, J. Simultaneous determination of bisphenol A and its halogenated derivatives in river water by combination of isotope imprinting and liquid chromatography−mass spectrometry. *J. Chromatogr. A* **2006**, *1134*, 16−23.

(2) Huang, N.; Liu, M.; Li, H.; Zhang, Y.; Yao, S. Synergetic signal amplification based on electrochemical reduced graphene oxide-ferrocene derivative hybrid and gold nanoparticles as an ultra-sensitive detection platform for bisphenol A. *Anal. Chim. Acta* **2015**, *853*, 249−257.

(3) Dong, X.; Qi, X.; Liu, N.; Yang, Y.; Piao, Y. Direct electrochemical detection of bisphenol A using a highly conductive graphite nanoparticle film electrode. *Sensors* **2017**, *17*, 836.

(4) Chung, E.; Jeon, J.; Yu, J.; Lee, C.; Choo, J. Surface-enhanced raman scattering aptasensor for ultrasensitive trace analysis of bisphenol A. *Biosens. Bioelectron.* **2015**, *64*, 560−565.

(5) Reza, K. K.; Ali, M. A.; Srivastava, S.; Agrawal, V. V.; Biradar, A. M. Tyrosinase conjugated reduced graphene oxide-based bio interface for bisphenol A sensor. *Biosens. Bioelectron.* **2015**, *74*, 644−651.

(6) Pellerin, E.; Caneparo, C.; Chabaud, S.; Bolduc, S.; Pelletier, M. Endocrine-disrupting effects of bisphenols on urological cancers. *Environ. Res.* **2021**, *195*, No. 110485.

(7) Gao, Y.; Cao, Y.; Yang, D.; Luo, X.; Tang, Y.; Li, H. Sensitivity and selectivity determination of bisphenol A using SWCNT−CD conjugate modified glassy carbon electrode. *J. Hazard. Mater.* **2012**, *199−200*, 111−118.

(8) Wu, L.; Deng, D.; Jin, J.; Lu, X.; Chen, J. Nanographene-based tyrosinase biosensor for rapid detection of bisphenol A. *Biosens. Bioelectron.* **2012**, *35*, 193−199.
(9) Cosio, M. S.; Pellicanò, A.; Brunetti, B.; Fuenmayor, C. A. A simple hydroxylated multi-walled carbon nanotubes modified glassy carbon electrode for rapid amperometric detection of bisphenol A. *Sens. Actuators, B* **2017**, *246*, 673−679.
(10) Ye, Z.; Wang, Q.; Qiao, J.; Ye, B.; Li, G. Simultaneous detection of bisphenol A and bisphenol S with high sensitivity based on a new electrochemical sensor. *J. Electroanal. Chem.* **2019**, *854*, No. 113541.
(11) ten Cate, A. T.; Sijbesma, R. P. Coils, rods and rings in hydrogen-bonded supramolecular polymers. *Macromol. Rapid Commun.* **2002**, *23*, 1094−1112.
(12) Beck, J. B.; Ineman, J. M.; Rowan, S. J. Metal/Ligand-induced formation of metallo-supramolecular polymers. *Macromolecules* **2005**, *38*, 5060−5068.
(13) Patra, G. K.; Goldberg, I. Supramolecular design of coordination complexes of silver(I) with polyimine ligands: synthesis, materials characterization, and structure of new polymeric and oligomeric materials. *Cryst. Growth Des.* **2003**, *3*, 321−329.
(14) Islam, T.; Hasan, M.; Akter, S. S.; Alharthi, N. H.; Karim, M. R.; Aziz, A.; Hossain, M. D.; Ahammad, A. J. S. Fabrication of Ni-Co-based heterometallo-supramolecular polymer films and the study of electron transfer kinetics for the nonenzymatic electrochemical detection of nitrite. *ACS Appl. Polym. Mater.* **2020**, *2*, 273−284.
(15) Aida, T.; Meijer, E. W.; Stupp, S. I. Functional supramolecular polymers. *Science* **2012**, *335*, 813−817.
(16) Yu, G.; Yan, X.; Han, C.; Huang, F. Characterization of supramolecular gels. *Chem. Soc. Rev.* **2013**, *42*, 6697−6722.
(17) Nia, N. Y.; Farahani, P.; Sabzyan, H.; Zendehdel, M.; Oftadeh, M. A combined computational and experimental study of the $[Co(bpy)_3]^{2+/3+}$ complexes as one-electron outer-sphere redox couples in dye-sensitized solar cell electrolyte media. *Phys. Chem. Chem. Phys.* **2014**, *16*, 11481−11491.
(18) Elgrishi, N.; Chambers, M. B.; Artero, V.; Fontecave, M. Terpyridine complexes of first row transition metals and electrochemical reduction of CO_2 to CO. *Phys. Chem. Chem. Phys.* **2014**, *16*, 13635−13644.
(19) Pandey, R. K.; Hossain, M. D.; Moriyama, S.; Higuchi, M. Ionic conductivity of Ni(II)-based metallo-supramolecular polymers: effects of ligand modification. *J. Mater. Chem. A* **2013**, *1*, 9016−9018.
(20) Maier, A.; Rabindranath, A. R.; Tieke, B. Coordinative supramolecular assembly of electrochromic films based on metal ion complexes of polyiminofluorene with terpyridine substituent groups. *Chem. Mater.* **2009**, *21*, 3668−3676.
(21) Hu, L.; Fong, C. C.; Zhang, X.; Chan, L. L.; Lam, P. K. S.; Chu, P. K.; Wong, K. Y.; Yang, M. Au nanoparticles decorated TiO_2 nanotube arrays as a recyclable sensor for photo-enhanced electrochemical detection of bisphenol A. *Environ. Sci. Technol.* **2016**, *50*, 4430−4438.
(22) Beitollahi, H.; Moghaddam, H. M.; Tajik, S. Voltammetric determination of bisphenol A in water and juice using a lanthanum (III)-doped cobalt (II, III) nanocube modified carbon screen-printed electrode. *Anal. Lett.* **2019**, *52*, 1432−1444.
(23) Guo, Y.; Sun, Y.; Wang, Y.; He, H.; Zhu, Y. Thiol- and alkyne-functionalized copper nanoparticles as electrocatalysts for bisphenol A (BPA) oxidation. *J. Solid State Electrochem.* **2019**, *23*, 91−100.
(24) Bas, S. Z.; Yuncu, N.; Atacan, K.; Ozmen, M. A comparison study of MFe_2O_4 (M: Ni, Cu, Zn)-reduced graphene oxide nanocomposite for electrochemical detection of bisphenol A. *Electrochim. Acta* **2021**, *386*, No. 138519.
(25) Hossain, M. D.; Zhang, J.; Pandey, R. K.; Sato, T.; Higuchi, M. A heterometallo-supramolecular polymer with Cu^{I} and Fe^{II} Ions introduced alternately. *Eur. J. Inorg. Chem.* **2014**, *2014*, 3763−3770.
(26) Gellerman, G.; Rudi, A.; Kashman, Y. The Biornimetic Synthesis of marine alkaloid related fyrido- and pymolo[2,3,4-kl]acridines. *Tetrahedron* **1994**, *50*, 12959−12972.
(27) Yang, D.; Li, Z.; He, L.; Deng, Y.; Wang, Y. Solvent free mechanochemical synthesis of Eu^{3+} complex and its luminescent sensing of trace water and temperature. *RSC Adv.* **2017**, *7*, 14314−14320.
(28) Leung, J. J.; Warnan, J.; Ly, K. H.; Heidary, N.; Nam, D. H.; Kuehnel, M. F.; Reisner, E. Solar-driven reduction of aqueous CO_2 with a cobalt bis(terpyridine)-based photocathode. *Nat. Catal.* **2019**, *2*, 354−365.
(29) Awal, A.; Mia, M. M.; Sarkar, S.; Islam, S.; Sarker, S.; Nayem, S. M. A.; Hossain, M. D.; Ahammad, A. J. S. Fe (II)-based metallo-Supramolecular polymer film for electrochemical detection of nitrite: studies of kinetics and reaction mechanisms. *J. Electrochem. Soc.* **2023**, *170*, No. 037508.
(30) Awal, A.; Sarker, S.; Mia, M.; Hossain, M. D.; Ahammad, A. J. S. Fe(II)-based metallo-supramolecular polymer film as a sensing material for the detection of nitrite. *ECS Trans.* **2022**, *107*, 14783.
(31) Hasan, M. M.; Islam, T.; Imran, A.; Alqahtani, B.; Shaheen, S.; Mahfoz, W.; Rezaul, M.; Alharbi, H. F.; Aziz, A.; Ahammad, A. J. S. Mechanistic insights of the oxidation of bisphenol A at ultrasonication assisted polyaniline-Au nanoparticles composite for highly sensitive electrochemical sensor. *Electrochim. Acta* **2021**, *374*, No. 137968.
(32) Yin, H.; Zhou, Y.; Ai, S.; Han, R.; Tang, T.; Zhu, L. Electrochemical behavior of bisphenol A at glassy carbon electrode modified with gold nanoparticles, silk fibroin, and PAMAM dendrimers. *Microchim. Acta* **2010**, *170*, 99−105.
(33) Zhang, J.; Li, Q.; Chen, M.; Li, H.; Xu, Z. Electrochemically monitoring the removal of bisphenol A based on its anodic deposition at an ITO electrode. *Sens. Actuators, B* **2011**, *160*, 784−790.
(34) Yu, C.; Gou, L.; Zhou, X.; Bao, N.; Gu, H. Chitosan−Fe_3O_4 nanocomposite based electrochemical sensors for the determination of bisphenol A. *Electrochim. Acta* **2011**, *56*, 9056−9063.
(35) Lin, Y.; Liu, K.; Liu, C.; Yin, L.; Kang, Q.; Li, L.; Li, B. Electrochemical sensing of bisphenol A based on polyglutamic acid/amino-functionalised carbon nanotubes nanocomposite. *Electrochim. Acta* **2014**, *133*, 492−500.
(36) Koyun, O.; Gorduk, S.; Gencten, M.; Sahin, Y. A novel copper(II) phthalocyanine-modified multiwalled carbon nanotube-based electrode for sensitive electrochemical detection of bisphenol A. *New J. Chem.* **2019**, *43*, 85−92.
(37) Zou, J.; Liu, Z.; Guo, Y.; Dong, C. Electrochemical sensor for facile detection of trace bisphenol A based on cyclodextrin functionalized graphene/platinum nanoparticles. *Anal. Methods* **2017**, *9*, 134−140.
(38) Liang, H.; Zhao, Y.; Ye, H.; Li, C. P. Ultrasensitive and ultrawide range electrochemical determination of bisphenol A based on PtPd bimetallic nanoparticles and cationic pillar[5] arene decorated graphene. *J. Electroanal. Chem.* **2019**, *855*, No. 113487.
(39) Ali, H.; Mukhopadhyay, S.; Jana, N. R. Selective electrochemical detection of bisphenol A using a molecularly imprinted polymer nanocomposite. *New J. Chem.* **2019**, *43*, 1536−1543.
(40) Ling, L. J.; Xu, J. P.; Deng, Y. H.; Peng, Q.; Chen, J. H.; He, Y. S.; Nie, Y. J. One pot hydrothermal synthesis amine-functionalized metal-organic framework/reduced graphene oxide composites for electrochemical detection of bisphenol A. *Anal. Methods* **2018**, *10*, 2722−2730.
(41) Qin, J.; Shen, J.; Xu, X.; Yuan, Y.; He, G.; Chen, H. A glassy carbon electrode modified with nitrogen-doped reduced graphene oxide and melamine for ultra-sensitive voltammetric determination of bisphenol A. *Microchim. Acta* **2018**, *185*, 459.
(42) Ben Messaoud, N.; Lahcen, A. A.; Dridi, C.; Amine, A. Ultrasound assisted magnetic imprinted polymer combined sensor based on carbon black and gold nanoparticles for selective and sensitive electrochemical detection of bisphenol A. *Sens. Actuators, B* **2018**, *276*, 304−312.
(43) Hasan, M. M.; Islam, T.; Akter, S. S.; Alharthi, N. H.; Karim, M. R.; Aziz, M. A.; Awal, A.; Hossain, M. D.; Ahammad, A. J. S. Computational approach to understanding the electrocatalytic reaction mechanism for the process of electrochemical oxidation of nitrite at a Ni−Co-based heterometallo-supramolecular polymer. *ACS Omega* **2020**, *5*, 12882−12891.

https://doi.org/10.1021/acsomega.3c02206
ACS Omega 2023, 8, 28355−28366

(44) Suen, N. T.; Hung, S. F.; Quan, Q.; Zhang, N.; Xu, Y. J.; Chen, H. M. Electrocatalysis for the oxygen evolution reaction: recent development and future perspectives. *Chem. Soc. Rev.* **2017**, *46*, 337−365.
(45) Hasan, M. R.; Islam, T.; Hasan, M. M.; Chowdhury, A. N.; Ahammad, A. J. S.; Reaz, A. H.; Roy, C. K.; Shah, S. S.; Al-Imran; Aziz, M. A. Evaluating the electrochemical detection of nitrite using a platinum nanoparticle coated jute carbon modified glassy carbon electrode and voltametric analysis. *J. Phys. Chem. Solids* **2022**, *165*, No. 110659.

https://doi.org/10.1021/acsomega.3c02206
ACS Omega 2023, 8, 28355−28366